Acquisition of Precise Probe Vehicle Data in Urban City Based on Three-Dimensional Map Aided GNSS

Yanlei Gu
The University of Tokyo,
Tokyo, Japan
guyanlei@kmj.iis.u-tokyo.ac.jp

Li-Ta Hsu
Hong Kong Polytechnic University,
Hong Kong, China
lt.hsu@polyu.edu.hk

Shunsuke Kamijo
The University of Tokyo,
Tokyo, Japan
kamijo@iis.u-tokyo.ac.jp

***Abstract*— Global Navigation Satellite System (GNSS) based vehicle probe technology is emerging as an effective means to monitor traffic flow and optimize traffic control. Moreover, the accuracy of the probe vehicle data is expected to be sub-meter level or even more precise for the lane-level traffic analysis. However, the performance of GNSS positioning technique is severely degraded in urban canyons, because the multipath effect and Non-Line-Of-Sight propagation. We proposed to rectify the positioning result of the commercial GNSS single frequency receiver using the three-dimensional building map, which is named 3D-GNSS. This paper proposes to employ the 3D-GNSS positioning method for the acquisition of the precise probe vehicle data. With the benefit of the proposed method, the global lane-level position, speed and stop state of vehicles are expected to be recognized from the 3D-GNSS based probe data. Finally, the accuracy of the 3D-GNSS based probe technology is evaluated in one of the most challenging urban city, Tokyo. The experiment results demonstrate that the proposed method can achieve 87% correct lane rate in the localization, and has sub-meter accuracy with respect to position and speed error mean. The accurate position and speed estimation provided by 3D-GNSS, result 92% correct rate in detecting stop vehicles.**

Keywords—GNSS; 3D building map; Probe data; Vehicle localization

I. INTRODUCTION

As urban populations increase, existing and emerging cities face the challenge of meeting rising demands for efficient mobility within limited physical infrastructure capacity. Simultaneously, citizens' expectations are changing continually, influenced by ongoing innovations around Intelligent Transportation Systems (ITS). Global Navigation Satellite System (GNSS) based vehicle probe technology is emerging as an effective means for traffic control and city development. The probe data, which includes vehicle position, speed, time, and other information, offers the potential to develop transformative applications that can improve roadway operations, planning, and maintenance, and keep travelers informed of travel conditions [1-3]. The accuracy of the vehicle localization in the probe data is expected to be sub-meter level or even more precise for the lane-level traffic analysis [4].

Currently, the most of the accurate vehicle localization systems employ high cost measurement devices, such as Velodyne or stereo camera [5-7]. However, a low cost collection device is more popular in the vehicle probe industry for increasing the number of equipped vehicles and enlarging the monitored area in urban city. Currently, the commercial level GNSS receiver and accelerometer are already available in the probe data collection devices. Thus, this paper focuses on improving the quality of the probe vehicle data based on GNSS positioning method and the available accelerometer sensor.

GNSS is developed as a positioning technology, and is widely used in various daily-use devices such as vehicle navigators and cell phones. However, the GNSS receiver embedded in commercial device is usually low-cost, single-frequency with stand-alone modules. The single frequency GNSS receiver has a satisfactory positioning performance in open fields. However, its positioning performance is severely degraded in urban canyons. The main reason is the multipath effect and Non-Line-Of-Sight (NLOS) propagation. These effects may lead to a positioning error of around 100 meters in urban canyons [8].

Many sophisticated algorithms were developed to mitigate the effects caused by multipath and NLOS effect, such as vehicular communication [9], omnidirectional infrared camera [10], shadow matching [11] and Three-Dimensional (3D) building model [12]. Our research team proposed a candidate distribution based positioning method using 3D building map. The evaluation in our previous works demonstrated that the developed 3D map aided GNSS (3D-GNSS) positioning method achieved high performance in urban canyon environments [13, 14]. Considering the available sensors for autonomous vehicle applications, we further integrated 3D-GNSS with Inertial Measurement Unit (IMU), speedometer [15] and on-board camera [16, 17]. The integrated localization system achieved sub-meter accuracy with respect to positioning error mean in the urban environment.

The accelerometer has been widely used to recognize the type of the driving events (e.g. brake, lane change, etc.) and driving styles [18]. In addition, the classification of the different driving events was also performed based on the data collected from the accelerometer in smartphones [19]. The algorithm proposed in [20] relies on both accelerometer and gyroscope. Moreover, the accelerometer and GNSS receiver in smartphones were used together to monitor road and traffic conditions, to detect potholes, bumps as well as vehicles braking and honking [21]. These papers proved the effectiveness of accelerometers in the driving event detection.

The following publication Y. Gu, L. Hsu and S. Kamijo, "Acquisition of precise probe vehicle data in urban city based on three-dimensional map aided GNSS," 2017 IEEE 20th International Conference on Intelligent Transportation Systems (ITSC), 2017, pp. 1-7 is available at https://doi.org/10.1109/ITSC.2017.8317776.

The first contribution of this paper is to introduce the 3D-GNSS method to the vehicle probe research field, and comprehensively evaluate the effectiveness of the 3D-GNSS based probe technology for lane-level traffic analysis. The evaluation includes both the position and speed domains. The second contribution is the development of a stopping vehicle detection, which could be used to recognize the congestion situation in each vehicle lane. The third contribution is to employ the accelerometer sensor for improving the correct lane rate of the positioning results estimated from the standalone GNSS technique. These three contributions are described in Sections II and III. The experimental result will be demonstrated in Section IV. Finally, this research is concluded and discussed in Section V.

II. Three-Dimensional Map aided GNSS Positioning

In the urban environment, the effects of multipath and NLOS are the main reason for the pseudorange measurement error. To reduce both multipath and NLOS effects, 3D-GNSS utilizes ray-tracing algorithm and 3D building map to simulate the reflecting path of satellite signal transmission. The detailed description of the algorithm of 3D-GNSS has been published in our previous works [13-17].

Figure 1 demonstrates the schematic of 3D-GNSS with differential correction. A reference station is installed to receive the GNSS measurements. The position of reference station is fixed and previously surveyed using precise point positioning (PPP) or other approaches. After the generating a differential correction, the correction is transmitted to rover. The rover then employs it to the common satellites in view to improve its own positioning accuracy. Theoretically, when the differential positioning for the distance between the reference and rover station is within 50 km, the ionospheric delay, tropospheric delay, satellite clock error, and satellite orbit error of the rover station can be eliminated by applying differential correction. As the result, the positioning error of the rover station is mainly caused by the multipath and NLOS effects.

In 3D-GNSS, 3D building map and ray-tracing is used for estimating the pseudorange delay and reducing the multipath and NLOS effects. Figure 1 shows an example of the ray-tracing result. With this idea, the 3D-GNSS distributes position candidates around the raw position provided by conventional GNSS receiver and previous positioning result. Ideally, if the position of a candidate locates at the true position, the difference between the simulated and observed pseudoranges (Pr.) should be zero. Finally, the 3D-GNSS method provides an optimal positioning result by considering the similarity of the simulated pseudoranges of each candidate and observed pseudoranges. As shown in Figure 1, connected with the step "Calculation of Pos. Result", the candidates in the vicinity of the ground truth have higher probability for positioning. This example demonstrates that the 3D map information is effective for reducing the effects of multipath and NLOS.

III. Acquisition of Precise Probe Vehicle Data

In the acquisition of the probe vehicle data, the vehicle position is estimated from the 3D-GNSS method. Moreover, the vehicle speed is directly calculated from the positioning

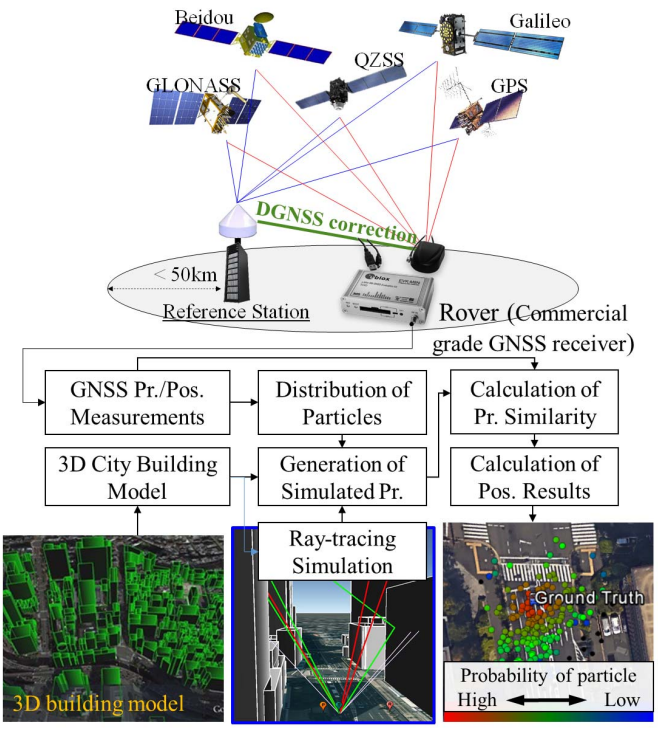

Fig. 1. Flowchart of 3D-GNSS with differential correction [14].

results based on the distance between two consecutive epochs. Based on the position and speed information, the stop detection and lane-level localization system is developed.

A. Stop Detection using Estimated Speed from 3D-GNSS

Vehicle speed is a continuous value to describe the status of vehicles. Discrete description of vehicle state, such as stop or not, is also significant for traffic analysis. We expect that the stop state can be recognized correctly using speed information estimated from 3D-GNSS. Generally, it is difficult to choose a constant threshold to distinguish stop from drive event. Thus, we propose to use the probabilistic estimation method for stop detection. Dynamic Bayesian Network (DBN) has been widely used for sequential data analysis, such as pedestrian and driver behavior analysis [22]. This paper also uses the DBN model to recognize whether the vehicle is stopped or not. In addition, we use particle filter as the inference technique in this model. The proposed DBN model is shown in Figure 2.

The square with text D_t denotes the decision about stop at time t. It connects with the ellipse S_{t-1}, the estimated speed at time t-1. It means that the probability of stop depends on the value of the estimated speed at the previous epoch. In addition, the estimated speed note S_t is connected with the decision note D_t and speed note S_{t-1}. This design can explain the relationship of the speed change in different events. For example, in the stop case, the speed should not change, but the speed may change in drive because of the acceleration or deceleration. Moreover, the speed note S_t is connected with the gray ellipse Z_t, observation note. This connection denotes how confident the estimated speed is compared to the observed speed. This connection is used to evaluate the weight of each particle.

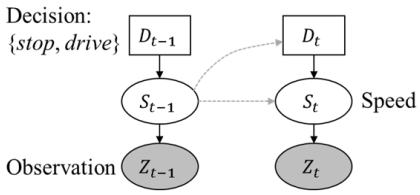

Fig. 2. Proposed Dynamic Bayesian Network model for stop detection.

Based on the structure of the proposed DBN mode, the probability of stop for each particle can be formulated as:

$$P(D_t, S_t \mid S_{t-1}) = P(D_t \mid S_{t-1}) P(S_t \mid S_{t-1}, D_t) \quad (1)$$

$$P(D_t \mid S_{t-1}) = \frac{1}{1+\exp(-(\alpha+\beta S_{t-1}))} \quad (2)$$

$$P(S_t \mid S_{t-1}, D_t) \propto \exp\left(-\frac{\left(\left(S_t - S_{t-1}\right) - \mu_{D_t}\right)^2}{2\sigma_{D_t}^{\ 2}}\right) \quad (3)$$

where, $P(D_t \mid S_{t-1})$ is a logistic function, α and β are the learned parameters, which can explain the relationship between the speed and stop event. The left image in Figure 3 visualizes the two parameters using the training data. The blue points correspond to the drive, and red points mean the stop data, the curve represents the learned model which is described in equation (2). We can see that the lower speed data has higher probability for stop, and higher speed data indicates lower probability for stop. In other words, the learned model has the good performance to recognize the stop and drive using speed information.

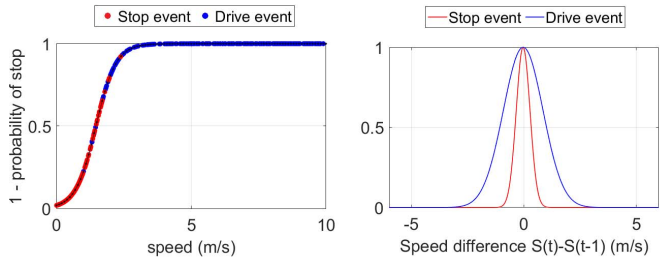

Fig. 3. Visualization of learned parameters for DBN model of stop detection.

$P(S_t \mid S_{t-1}, D_t)$ is defined as a context Gaussian function, which has different parameters for the stop and drive contexts. The explanatory variable in the Gaussian function is speed change $S_t - S_{t-1}$ from the last epoch the current epoch. μ_{D_t} and σ_{D_t} are the learned parameters from training data. The right image in Figure 3 visualizes the distribution of the speed change $S_t - S_{t-1}$, which represents the μ_{D_t} and σ_{D_t} as well. It is clearly see that the red curve is a narrow distribution, which means that the speed change in stop context is relative small but does not only concentrate on the position of zero. The reason is that GNSS based positioning results could not be fixed in a constant position even if a vehicle stops because of the positioning error. However, the speed change in drive situation is greater than that in stop, because the speed change caused by both the positioning error and the vehicle acceleration. Equations (1) to (3) are used for the estimation of the probability to stop of each particle.

Because this paper adopts the particle filter as the inference, the probability of stop decision at time t can be formulated as:

$$P(D_t) = \sum_{i=1}^{n} W_t^i \cdot P(D_t^i \mid S_{t-1}^i) \quad (4)$$

$$W_t^i = P(Z_t \mid S_t^i) = \exp\left(-\frac{\left(S_t^i - Z_t\right)^2}{2\sigma^2}\right) \quad (5)$$

where, W_t^i is the weight of each particle, i is the index of particles. Z_t is the speed calculated from GNSS positioning result at time t, σ is empirically setup as 1 m/s in this research. Equation (5) means that the more similar the estimated speed S_t and the observed speed Z_t are, the higher weight the particle has. The accuracy of the stop detection will be illustrated in Section IV

B. Lane-Level Localization by 3D-GNSS and Accelerometer

This research also proposes to use on-board accelerometer to detect lane-change and lane-keep event. The lane-change and lane-keep event can be used to rectify the positioning error of GNSS positioning result by referring to the 2D map with lane information. The accelerometer is attached on the floor of the vehicle. The X axis of the accelerometer is the heading direction of the vehicle. The Y axis directs to right side of the vehicle. Thus, the Z axis points down. The acceleration value along the Y axis is used for lane-change detection in this research.

In order to distinguish the lane-change from non-lane-change, we need to exclude the turning and lane-keep behaviors. The turning behaviors happen in the intersections or the road areas with curvature. Thus, we could specify these areas in the road map. Our propose method determines that the lane-change will not be detected when GNSS positioning results are in these areas. After that, we use the template matching based method to distingush the lane-change from lane-keep behaviors.

In order to get a template to represent the pattern, we collect multiple samples for the lane-change events. In this research, we use the right-direction lane-change as the example to explain the method. The collected samples are firstly centralized, and normalized along the time direction (horizontal axis) in order to make the samples have the same time length. After that, the samples are normalized along the acceleration direction (vertical axis). The purpose of the centralization and normalizations is to make the pattern become obvious. The centralized and normalized samples are shown in Figure 4 (a). Each colored curve denotes one lane-change event. Then, the curve fitting method is used to learn the pattern of the acceleration in lane-change event, as shown in Figure 4 (b).

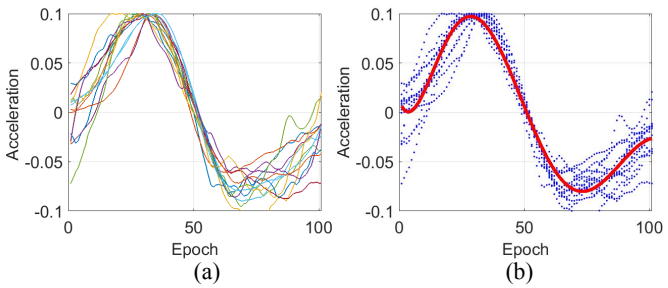

Fig. 4. (a) Centralized and normalized Y direction acceleration for multiple lane-change events, (b) Curve fitting using acceleration data from multiple lane-change events, the red curve is the learned template using curve fitting.

After we have the template, the sliding window method is used for template matching. First, the data within a time window is extracted. Then, the normalizations are conducted along the horizontal and vertical directions, respectively. This data is called test data. After that, the correlation coefficient between the test data and learned template is used to find the candidates of lane-change events. Correlation can be formulated as follows:

$$C(T,L)=\frac{1}{N-1}\sum_{i=1}^{N}\left(\frac{T_i-\mu_T}{\sigma_T}\right)\left(\frac{L_i-\mu_L}{\sigma_L}\right) \tag{6}$$

where, μ_T and σ_T are the mean and standard deviation of test event data, respectively, and μ_L and σ_L are the mean and standard deviation of the learned template. N is the length of the data. T_i and L_i are the ith point in test and template data, respectively. Figure 5 shows the correlation result on a data with 5-minute length. In this period, the acceleration on Y direction changes according to different driving events, as shown by the green curve. The correlation result is indicated by

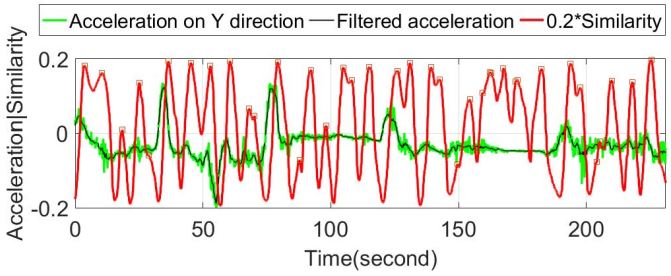

Fig. 5. Pattern matching result on test data using correlation with the learned template.

the red curve, this curve is scaled by a factor 0.2 for visualization. We can observe that there are several peaks. The acceleration around of the peaks indicates there is a similar pattern to the learned template of lane-change event. We also understand that only using the similarity estimated by the correlation is not enough to accurately recognize the lane-change event because there are many detected peaks.

In order to detect the lane-change events correctly, we propose to use one more feature, which is the variance of acceleration in a local time window. We call it acceleration variance in this research. The acceleration variance can be described as follows:

$$V_t=\max A-\min A \quad A\in\{A_{t-k},A_{t+k}\} \tag{7}$$

where, $\max A$ is the maximum acceleration in the time window $(t-k,t+k)$, and $\min A$ is the minimum acceleration. We use the similarity estimated by the correlation and the acceleration variance together to recognize lane-change events from the candidates provided by only using the correlation.

In order to learn the joint relationship between the acceleration variance, correlation similarity and probability of lane-change, we select 100 training data, which includes both lane-change and other events. Because this step only focuses on the candidates provided by correlation step, we chose the data which has the peaks in the template matching process for the training. The two classes: lane-change and non-lane-change, are expected to be separated by using the learned model. We propose to use logistic regression to learn the joint relationship. The model is described as follows:

$$P(laneChange\,|\,\{A_{t-k},A_{t+k}\})=\frac{1}{1+\exp\left(-(\alpha+\beta_1V_t+\beta_2C_t)\right)} \tag{8}$$

Where, α, β_1 and β_2 are the learned parameters. V_t and C_t are the acceleration variance and correlation similarity, which are defined in equation (7) and (6), respectively. Figure 6 shows the training data and logistic regression result. The blue points are corresponding to the lane-change, and red points mean the non-lane-change data, the curving surface represents the learned model. The color on the surface denotes the probability of lane-change. We can see that the learned model has the good performance for recognizing the lane-change and non-lane-change. We will use this model to decide whether the candidate is lane-change or not.

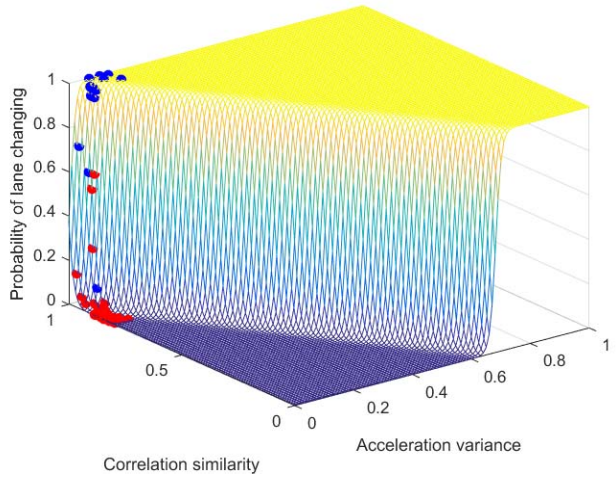

Fig. 6. Two-dimensional logistic regression for lane-change recognition. Blue points are the lane-change data,red points is the non-lane-change data, the curving surface is the representation of the logistic regression result.

Figure 7 shows the recognition result of lane-change using pattern similarity and acceleration variance. Similar to Figure

5, the correlation result is indicated by the red curve, this curve is scaled by 0.2 factor for visualization. We can observe that there are several peaks. Then we apply the learned model, which has been shown in Figure 6, to each peak to judge whether the peak is lane-change or not. The red points are the probability of lane-change for the peak candidates. This probability has been scaled by 0.3 for visualization. It is clear to see that the most of the peaks have low probability and only three peaks have high probability, which are close to 1. These three peaks are in areas of the lane-change events.

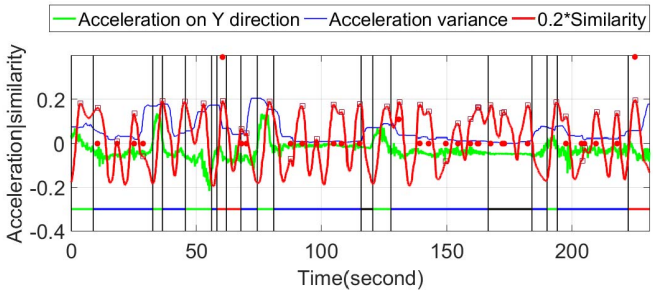

Fig. 7. Lane-change detection. The green curve is the acceleration on Y direction, red curve is the correlation result with 0.2 scaling factor for visualization, blue curve is the variance of acceleration in a time window. The lines at -0.3 indicate the ground truth of the type of behavior (blue: lane-keep, black: stop, green: turning, red: lane-change), the red points denote the probability of lane-change.

If the system does not detect the lane-change behavior in one road link. GNSS positioning results will be rectified by finding the minimum distance from GNSS trajectory to each possible lane center which is included in road map. Figure 8 shows one example for the rectification of the GNSS positioning results. The red points are the positioning results provided by 3D-GNSS method. The red lines are the lane centers. The red line with x label is the lane, in which the vehicle was driven. The blue squares are the rectified positioning results. Because the most of the red points are in the correct lane and the accelerometer also indicates that there is no lane-change event, we could rectify the several red points in the neighboring lane to the correct lane. When the lane-change is detected, this rectification method also can be used for improving the correct lane rate.

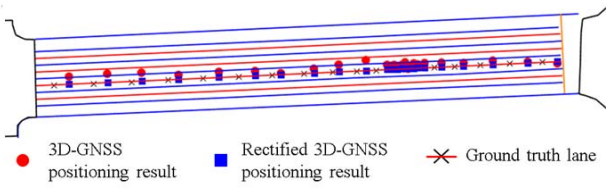

Fig. 8. Rectification for GNSS positioning results using road map and lane-change recognition.

IV. Experiments

The proposed 3D-GNSS was evaluated in the experiments conducted around Hitotsubashi area in Tokyo. We chose this place for experiments due to the density of tall buildings. Figure 9 shows the developed 3D building map, 2D lane-level road map and the experimental devices for this research. In the experiment, a u-blox EVK-M8 GNSS model, a commercial level receiver was adopted. It can receive signals from multiple-GNSS (GPS, GLONASS, and QZSS). We placed the u-blox receiver on the top of our vehicle to collect pseudorange measurements. We setup the reference station in the roof of our research building, which is the highest building in the surrounding area. The baseline between the reference station and experiment area is less than 20 kilometers. The output rate of both receivers is 1 Hz. Beside the GNSS receiver, the speedometer and accelerometer were equipped in the vehicle for obtaining the vehicle velocity and acceleration. Moreover, an onboard camera, which captured the front view images, was installed in the vehicle as well. The data from these sensors were synchronized in the experiments.

The driving distance is approximately 1500 meters in each test. In the vehicle self-localization, it is more important to distinguish which lane the vehicle is in compared to the positioning accuracy. Therefore, both the lateral error and the correct lane rate are employed to estimate the performance of the localization system. We manually distinguished the ground truth trajectory of our vehicle from these images, and manually decided the occupied lane for the result evaluation by referring to the onboard camera and a high-resolution aerial image. In addition, the ground truth of stop, drive, lane-change and lane-keep was also obtained from the on-board camera. The ground truth of speed was obtained from vehicle speedometer data. We also optimize the speed value in the low speed situation using the camera. For example, we set the speed value as zero when the car stops, which is observed from the camera.

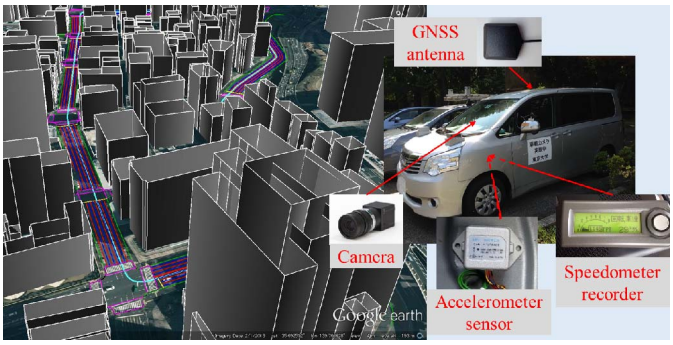

Fig. 9. 3D building map, 2D lane-level road map and the experimental devices used in this research.

A. Evaluation for Localization Accuracy

In order to understand the benefit of the proposed 3D-GNSS in urban canyon environments, this paper compares 3D-GNSS with the widely used Weighted Least Square (WLS) GNSS. The results are evaluated from different aspects, including positioning error, availability and correct lane rate. The correct lane rate indicates how many percent of localization results are the same as the lane, in which we drove in the experiment. For example, we drove at the second lane for 100 seconds in the experiment, and the localization results also indicated that the vehicle was in the second lane for 92

seconds. In this case, the result of the correct lane rate will be 92%. Availability means how many epochs have results in 100 epochs. Table 1 shows the quantitative evaluation. As indicated in Table 1, the developed 3D-GNSS has 1.09 meter positioning error, and provides 74.8% of correct lane rate in the urban area. However, the WLS-GNSS, which is the conventional method, has 4.72 meter positioning error and only provides 23.8% correct lane rate. In order to understand how much the proposed method can improve the performance compared to WLS-GNSS, one experiment result is visualized on Google Earth, as shown in Figure 10. WLS-GNSS results, and 3D-GNSS results are indicated by green and red color. The cyan line is the ground truth. It is clear to see that the positioning results of 3D-GNSS method are much more accurate compared to WLS-GNSS.

TABLE I. COMPARISON OF DIFFERENT GNSS POSITIONING METHODS

Positioning methods	*Positioning error mean (m)*	*Positioning error std. (m)*	*Availability*	*Correct lane rate*
WLS-GNSS	4.72	4.88	95.3%	23.8%
3D-GNSS	1.09	0.86	96.8%	74.8%
3D-GNSS & lane-change detection	0.51	0.82	96.8%	87.1%

This paper also proposes to use accelerometer to detect the lane-change event, and improve the position error and correct lane rate of localization. 75% lane-change events can be correctly recognized and there is no incorrect recognition for lane-keep events. The three cases are demonstrated in Figure 11 to show the effectiveness of the rectification. Case (a) and (b) are the lane-keep events. Because most GNSS positioning results are in the correct lanes, the rectification can improve the correct lane rate of localization in (b). However, the Figure 11 (a) shows the failed case. But the number of this kind of case is less than that of successful cases in all experiments, thus the total correct lane rate is improved. In addition, case (c) shows the lane-change event. Because the successful detection of lane-change from accelerometer, the positioning results also can be rectified based on the lane-change moment. Finally, the correct lane rate can be improved to 87.1%. The positioning error is also reduced to 0.51 meter, as shown in Table I.

Fig. 10. Visualization of positioning results of GNSS positioning methods.

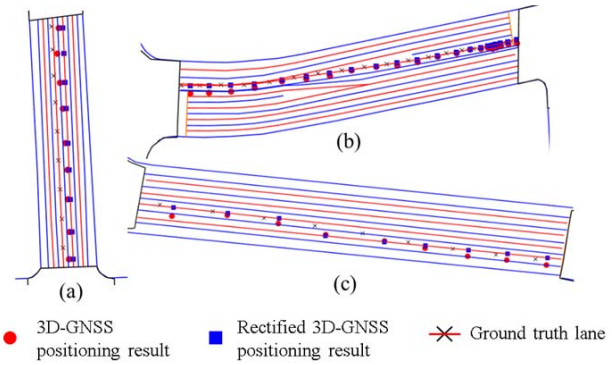

Fig. 11. Three cases of the rectification for GNSS positioning results using road map and lane-change recognition.

B. *Evaluation for Speed Error and Stop Detection*

Figure 12 shows the speed estimation and stop detection results from WLS-GNSS and 3D-GNSS, respectively. The blue line is the ground truth. The red line and green line in upper figure are the speed from 3D-GNSS and WLS-GNSS. Red line and green line in bottom figure indicate the probability for stop estimated from 3D-GNSS and WLS-GNSS, respectively. It is easy to recognize that 3D-GNSS based stop detection has better performance than that of WLS-GNSS based stop detection. The main reason is that the 3D-GNSS can provide more accurate speed. The WLS-GNSS is not reliable. For example, the speed and stop recognition result in the first stop area (around of 90) is totally wrong. Even though the speed calculation from WLS-GNSS in the fourth stop area becomes more accurate, the accuracy is not enough to distinguish the stop from drive. 3D-GNSS is more reliable compared to the WLS-GNSS in both stop and drive detection.

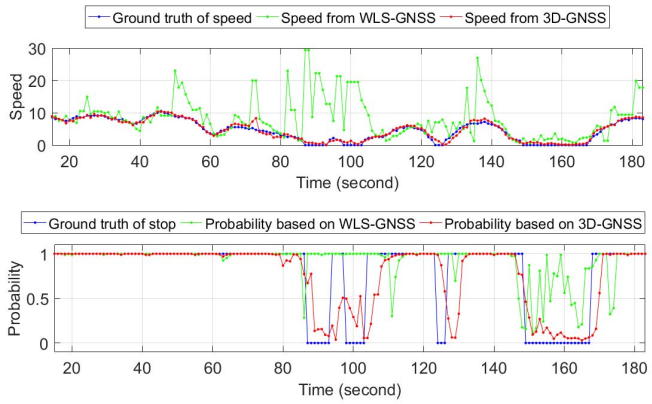

Fig. 12. Stop detection result using the speed calculated from GNSS.

As shown in Table II, speed error of 3D-GNSS is less than 1 m/s. It is much more accurate than WLS-GNSS based speed estimation. In addition, a comparison for stop detection is conducted between WLS-GNSS and 3D-GNSS as well. Table III shows the detection rate by using the two methods. In fact, both WLS-GNSS and 3D-GNSS have good performance for drive detection. But for the stop detection, the 3D-GNSS shows much better performance than that of WLS-GNSS. The reason is that the positioning results of WLS-GNSS also jump around the stop position, the speed from the jumping data shows a

similar value as drive. But 3D-GNSS shows very low speed value in the stop event. Therefore, 3D-GNSS has reliable and balanced performance for both stop and drive detection.

TABLE II. COMPARISON OF SPEED ESTIMATION FROM DIFFERENT GNSS POSITIONING METHODS IN URBAN AREAS

Positioning methods	*Speed error mean (m/s)*	*Speed error std. (m/s)*
WLS-GNSS	4.27	6.26
3D-GNSS	0.90	0.92

TABLE III. DETECTION RATE OF STOP AND DRIVE USING WLS-GNSS AND 3D-GNSS

WLS-GNSS based stop detection		***Real***	
		stop	***drive***
Estimation	***stop***	59.5%	3.4%
	drive	40.5%	96.6%

3D-GNSS based stop detection		***Real***	
		stop	***drive***
Estimation	***stop***	91.9%	5.9%
	drive	8.1%	94.1%

V. CONCLUSIONS AND FUTURE WORKS

One of the most important points in the city development is to improve the utilization rate of the vehicle lanes. This work needs to analyze the huge traffic data with accurate vehicle trajectories. More specific, lane-level localization accuracy is required for conducting this analysis. This paper proposes to use 3D-GNSS and accelerometer together to improve the positioning accuracy. We achieved 87.1% correct lane rate. With this accurate positioning results, the analysis for the lane utilization rate could achieve more precise results. In addition to the lane utilization rate, vehicle speed is another important parameter for traffic analysis. Because of the accurate positioning result of 3D-GNSS, the speed estimation just has 0.9 m/s error. This speed accuracy can be used to recognize whether the traffic is completely stopped or slowly move. By combining the positioning result and speed, the 3D-GNSS can be used to analyze the traffic situation of each lane, such as how many vehicles use this lane, how is the average speed of each lane, how often the congestion happens for each lane, and also the difference between the neighboring two lanes.

ACKNOWLEDGMENT

The authors acknowledge the Grant-in-Aid for Japan Society for the Promotion of Science (JSPS) Postdoctoral Fellowship for Oversea Researchers.

REFERENCES

[1] O Qing, L.B. Robert, J. W. C. Van Lint, P. H. Serge, "A theoretical framework for traffic speed estimation by fusing low-resolution probe vehicle data", IEEE Transactions on Intelligent Transportation Systems 12, no. 3, pp. 747-756, 2011.

[2] T. Seo, T. Kusakabe, Y. Asakura, "Traffic state estimation with the advanced probe vehicles using data assimilation", In Proceedings of 2015 18th IEEE International Conference on Intelligent Transportation Systems (ITSC), pp. 824-830, 2015.

[3] E. Jenelius, H. N. Koutsopoulos, "Travel time estimation for urban road networks using low frequency probe vehicle data," Transportation Research Part B: Methodological, no. 53, pp. 64-81,2013.

[4] S. Y. Rompis, M.Cetin, F. Habtemichael, "Probe vehicle lane identification for queue length estimation at intersections", Journal of Intelligent Transportation Systems, 2017.

[5] J. Choi, "Hybrid map-based SLAM using a Velodyne laser scanner", In Proceedings of 2014 17th IEEE International Conference on Intelligent Transportation Systems, pp. 3082-3087. 2014

[6] M. Schreiber, C. Knoppel, U. Franke, "Laneloc: Lane marking based localization using highly accurate maps", In Proceedings of Intelligent Vehicles Symposium 2013, pp. 449-454, 2013

[7] H. Lategahn, C. Stiller, "City GPS using stereo vision", In Proceeding of 2012 IEEE International Conference on Vehicular Electronics and Safety (ICVES), pp. 1-6, 2012

[8] G. MacGougan, G. Lachapelle, R. Klukas, K. Siu, L. Garin, J. Shewfelt, and G. Cox, "Performance analysis of a stand-alone high-sensitivity receiver", GPS Solutions, vol. 6, no. 3, pp. 179-195, Dec. 2002.

[9] Alam, N., Balaei, A.T., Dempster, A.G, "An instantaneous lane-level positioning using DSRC carrier frequency offset", IEEE Transactions on Intelligent Transportation Systems, vol. 13, no. 4, pp.1566-1575, 2012.

[10] J.I. Meguro, T. Murata, J.I. Takiguchi, Y. Amano, T. Hashizume, "GPS multipath mitigation for urban area using omnidirectional infrared camera", IEEE Transactions on Intelligent Transportation Systems, no. 10, 22-30, 2009.

[11] P. D. Groves, "Shadow matching: A new GNSS positioning technique for urban canyons", J. Navig., vol. 64, no. 3, pp. 417-430, 2011

[12] M. Obst, S. Bauer, P. Reisdorf, G. Wanielik, "Multipath detection with 3D digital maps for robust multi-constellation GNSS/INS vehicle localization in urban areas", In Proceedings of the IEEE Intelligent Vehicles Symposium 2012, Alcala de Henares, Spain, pp. 184-190, 2012.

[13] L.-T. Hsu, Y. Gu, S. Kamijo, "3D building model based pedestrian positioning method using GPS/GLONASS/QZSS and its reliability calculation", GPS Solutions, pp. 1-16, 2015.

[14] L.-T. Hsu, Y. Gu, S. Kamijo, "Autonomous driving positioning using building model and DGNSS", in Proceedings of Navigation Conference (ENC), 2016 European, pp. 1-7, 2016.

[15] Y. Gu, L. T. Hsu, S. Kamijo, "GNSS/on-board inertial sensor integration with the aid of 3D building map for lane-level vehicle self-localization in urban canyon", *IEEE Transactions on Vehicular Technology*, vol. 65, no. 6, pp. 4274-4287, 2016.

[16] Y. Gu, L.T. Hsu, S. Kamijo, "Passive sensor integration for vehicle self-localization in urban traffic environment", Sensors, vol. 15, no. 12, pp. 30199-30220, 2015.

[17] Y. Gu, L.T. Hsu, S. Kamijo, "Vehicle localization based on three-dimensional map aided global navigation satellite system", In Proceedings of Transportation Research Board 96th Annual Meeting (TRB), 2017.

[18] C.Saiprasert,, T. Pholprasit, S. Thajchayapong, "Detection of driving events using sensory data on smartphone", International Journal of Intelligent Transportation Systems Research, 15(1), pp.17-28. 2017.

[19] D.A. Johnson, M.M. Trivedi, "Driving style recognition using a smartphone as a sensor platform", In Proceedings of 2011 14th International IEEE Conference on Intelligent Transportation Systems (ITSC), pp. 1609-1615, 2011.

[20] P.Mohan, V.N.Padmanabhan R.Ramjee, "Nericell: rich monitoring of road and traffic conditions using mobile smartphones", In Proceedings of the 6th ACM conference on Embedded network sensor systems, pp. 323-336, 2008.

[21] M. Fazeen, B. Gozick, R. Dantu,M. Bhukhiya, M. C. González, M. C. "Safe driving using mobile phones", IEEE Transactions on Intelligent Transportation Systems, no. 13, 1462-1468., 2012.

[22] Y. Hashimoto, Y. Gu, L. T. Hsu, M. Iryo-Asano, S. Kamijo. "A probabilistic model of pedestrian crossing behavior at signalized intersections for connected vehicles", Transportation Research Part C: Emerging Technologies, no. 71, pp. 164-181, 2016.